Flux Ratios for Effects of Permanent Charges on Ionic Flows with Three Ion Species: Case Study (II)

Ning Sun[1] and Weishi Liu[2,*]

[1] *College of Science, National University of Defense Technology, No.1 Fuyuan Road, Changsha 410073, China;*
[2] *Department of Mathematics, University of Kansas, 1460 Jayhawk Blvd., Room 405, Lawrence 66045, USA.*

Abstract. In this paper, we study effects of permanent charges on ion flows through membrane channels via a quasi-one-dimensional classical Poisson-Nernst-Planck system. This system includes three ion species, two cations with different valences and one anion, and permanent charges with a simple structure, zeros at the two end regions and a constant over the middle region. For small permanent charges, our main goal is to analyze the effects of permanent charges on ionic flows, interacting with the boundary conditions and channel structure. Continuing from a previous work, we investigate the problem for a new case toward a more comprehensive understanding about effects of permanent charges on ionic fluxes.

1 Introduction

Electrodiffusion exhibits rich phenomena and plays a central role for many applications [7,11,12,14,29,30,34]. Ionic flow through ion channels is one of critical topics of physiology. Ion channels are large proteins embedded in cell membranes that provide pathways for electrodiffusion of ions (mainly Na^+, K^+, Ca^{2+} and Cl^-) between inside and outside of cells [21–25,52,60]. Thus, ion channels permit permeation and selectivity, and produce electric signals for cells to communicate with each other.

Ion channels are defined by their structural characteristics, channel shapes and permanent charge distributions, which are responsible for biological functions of ion channels. The shape of a typical channel could be approximated as a cylindrical-like domain,

---

Corresponding author. Email address: sunning16@mails.jlu.edu.cn (Sun N), wsliu@ku.edu (Liu W)

with a non-uniform cross-section area. Within an ion channel, amino acid side chains are distributed mainly over a relatively ¡°short¡± and ¡°narrow¡± portion of the channel, with acidic side chains contributing negative charges and basic side chains contributing positive charges. Permanent charges play a major role for controlling ionic flow properties, interacting with other important physical parameters, such as boundary concentrations, boundary potential and ion valences of ionic mixtures [1, 13, 15, 16, 31, 39, 40, 51, 54, 55, 62, 65, 66].

Due to the limitation of present experimental techniques, the most basic functions of ion channels such as permeation and selectivity are mainly extracted from the I-V relation measured experimentally (see, e.g., [4, 6, 9]). The I-V relation defines a functional response of the channel structure and boundary conditions (see display (1.7)) and is an input-output type information of an average effect of the full dynamics of ionic flows. Individual ionic fluxes carry more information than the I-V relation, but it is expensive and challenging to measure them [26, 31, 59]. A point is that it is still not possible to "measure/observe" internal dynamical behaviors of ionic flows, which makes it difficult to understand ion channel properties from experimental data due to extremely rich phenomena that can be created by the multi-scale feature and the nonlinear interplay among those physical parameters.

Mathematical modelings, analyses and numerical simulations of ion channel problems provide an alternative and complementary approach for explaining observed biological phenomena and discovering new ones. Poisson-Nernst-Planck (PNP) systems serve as basic primitive models for ionic flows through ion channels (see, e.g., [2, 3, 15, 18, 28–30, 34, 37, 38, 51, 62]). There have been a great deal successes in analyzing PNP models (see, e.g., [1–4, 17, 27, 28, 43, 45, 46, 48, 57, 61, 65, 66]), particularly, those by geometric singular perturbation (GSP) theory (see, e.g., [10, 16, 17, 31–33, 36, 39–42, 44–46, 56, 64–66]), which makes it possible to explain some effects of different parameters on the physical properties.

For ionic flows involving two ion species (one cation and one anion), effects of permanent charges have been extensively examined and important phenomena, some counterintuitive, were revealed [27, 33, 41, 65, 66]. In terms of flux ratios introduced in [41], major findings for flows of two ion species are as follows. Depending on boundary conditions, a positive permanent charge can enhance the anion flux while inhibiting that of cation, can enhance the fluxes of both anion and cation, can inhibit the fluxes of both anion and cation, but, cannot enhance the cation flux while inhibiting that of cation; and, independent of boundary conditions, a positive permanent charge always helps the flux of anion more than that of cation.

Recently there are several works on ionic flows with three ion species, two cation species with the same valence and one anion species, and some interesting results are obtained on competition of the two cations (see, e.g., [5, 63, 67]). These results on competition of the two cations are obtained with measurements that are different from flux ratios. However, for three ion species of different valences, the analysis on PNP system is very limited. In [57], the authors started to examine effects of small permanent charges

on ionic flows involving three ion species (two cations with different valences and one anion). They treated a case with equal chemical potential difference and discovered several new phenomena, particularly, in sharp contrast to two ion species cases, a positive permanent charge can enhance the flux of either one of the cation species more than the anion flux. A 3×3 matrix D_0 (see Section 2.2.1 below), determined implicitly by the fluxes associated to zero permanent charge, plays a crucial role for the study in [57]. The matrix D_0 always has a zero eigenvalue. The case studied in [57] concerns the situation when the other two eigenvalues σ_{10} and σ_{20} of D_0 are real. We consider, in this work, the case when σ_{10} and σ_{20} are a pair of complex conjugate eigenvalues and establish several abstract results – counterparts of those provided in [57]. In order to draw concrete results, we further conduct a detailed study when σ_{10} and σ_{20} are a pair of pure imaginary eigenvalues. In addition to some results that are consistent with those for the case studied in [57], our results show that, in this new case, small positive permanent charges can enhance only the flux of the cation species with the smaller valence more than that of the anion.

The paper is organized as follows. In the rest of this introduction, we recall the quasi-one-dimensional PNP model for ionic flows and the flux ratio for permanent charge effects on individual fluxes, and present the setup of our study. In Section 2, we briefly review the geometric singular perturbation theory developed for PNP models in [40, 44] and some relevant results from [57]. In Section 3 contains the new case study on the flux ratios for permanent charge effects. We conclude the paper with a brief summary in Section 4.

1.1 A quasi-one-dimensional PNP model for ion transports

For a mixture of n ion species, a quasi-one-dimensional PNP model ([43, 47]) is

$$\frac{1}{A(X)}\frac{\mathrm{d}}{\mathrm{d}X}\left(\varepsilon_r(X)\varepsilon_0 A(X)\frac{\mathrm{d}\Phi}{\mathrm{d}X}\right) = -e_0\left(\sum_{s=1}^{n} z_s C_s + \mathcal{Q}(X)\right)$$

$$\frac{\mathrm{d}\mathcal{J}_k}{\mathrm{d}X} = 0, \quad -\mathcal{J}_k = \frac{1}{k_B T}\mathcal{D}_k(X)A(X)C_k\frac{\mathrm{d}\mu_k}{\mathrm{d}X}, \qquad k=1,\cdots,n, \tag{1.1}$$

where $X \in [0,l]$ is the coordinate along the longitudinal axis of the channel, $A(X)$ is the area of cross-section of the channel at the location X, $\varepsilon_r(X)$ is the relative dielectric coefficient, ε_0 is the vacuum permittivity, e_0 is the elementary charge, $\mathcal{Q}(X)$ is the permanent charge density, k_B is the Boltzmann constant, T is the absolute temperature; Φ is the electric potential, and, for the k-th ion species, z_k is the valence (the number of charges per particle), C_k is the concentration, $\mathcal{J}_k(X)$ is the flux density through the cross-section over X, $\mathcal{D}_k$ is the diffusion coefficient, and μ_k is the electrochemical potential depending on Φ and C_k.

Equipped with system (1.1), a meaningful boundary condition for ionic flows through ion channels is, for $k=1,\cdots,n$,

$$\Phi(0)=\mathcal{V}, \quad C_k(0)=\mathcal{L}_k>0; \qquad \Phi(l)=0, \quad C_k(l)=\mathcal{R}_k>0. \tag{1.2}$$

We are interested in study the boundary value problem (BVP) (1.1) and (1.2) for understanding effects of permanent charges $\mathcal{Q}$ on ionic fluxes $\mathcal{J}_k$'s.

As in many mathematical analyses of the BVP (1.1) and (1.2) (see, e.g., [27,41,57,65, 66]), we will work with a dimensionless form. Let C_0 be a characteristic concentration of the problems, for example,

$$C_0 = \max_{1 \leq k \leq n} \left\{ \mathcal{L}_k, \mathcal{R}_k, \sup_{X \in [0,l]} |\mathcal{Q}(X)| \right\}.$$

Set

$$\mathcal{D}_0 = \max_{1 \leq k \leq n} \left\{ \sup_{X \in [0,l]} \mathcal{D}_k(X) \right\} \quad \text{and} \quad \hat{\varepsilon}_r = \sup_{X \in [0,l]} \varepsilon_r(X).$$

Let

$$x = \frac{X}{l}, \quad h(x) = \frac{A(X)}{l^2}, \quad \bar{\varepsilon}_r(x) = \frac{\varepsilon_r(X)}{\hat{\varepsilon}_r}, \quad \varepsilon^2 = \frac{\bar{\varepsilon}_r \varepsilon_0 k_B T}{e_0^2 l^2 C_0}, \quad \phi(x) = \frac{e_0}{k_B T} \Phi(X),$$

$$c_k(x) = \frac{C_k(X)}{C_0}, \quad Q(x) = \frac{\mathcal{Q}(X)}{C_0}, \quad \bar{J}_k = \frac{\mathcal{J}_k}{lC_0 \mathcal{D}_0}, \quad D_k(x) = \frac{\mathcal{D}_k(X)}{\mathcal{D}_0}, \quad \bar{\mu}_k = \frac{1}{k_B T} \mu_k.$$

In terms of the new variables, the BVP (1.1) and (1.2) becomes

$$\frac{\varepsilon^2}{h(x)} \frac{\mathrm{d}}{\mathrm{d}x} \left(\bar{\varepsilon}_r(x) h(x) \frac{d\phi}{dx} \right) = -\sum_{s=1}^{n} z_s c_s - Q(x),$$
$$\frac{\mathrm{d}\bar{J}_k}{\mathrm{d}x} = 0, \quad -\bar{J}_k = h(x) D_k(x) c_k \frac{\mathrm{d}\bar{\mu}_k}{\mathrm{d}x}, \qquad k = 1, \cdots, n,$$

(1.3)

with the boundary conditions at $x = 0$ and $x = 1$

$$\phi(0) = V = \frac{e_0}{k_B T} \mathcal{V}, \quad c_k(0) = l_k = \frac{\mathcal{L}_k}{C_0}; \qquad \phi(1) = 0, \quad c_k(1) = r_k = \frac{\mathcal{R}_k}{C_0}.$$

(1.4)

Remark 1.1. One has the following symmetry of the boundary value problem:
If $(\phi(x), c_k(x), \bar{J}_k)$ is a solution of (1.3) and (1.4), then

$$(\phi^*(x), c_k^*(x), \bar{J}_k^*) = (\phi(1-x), c_k(1-x), -\bar{J}_k)$$

is a solution of (1.1) with the boundary conditions

$$\phi(0) = -V, \quad c_k(0) = r_k; \qquad \phi(1) = 0, \quad c_k(1) = l_k.$$

For boundary conditions, to avoid sharp boundary layers [65,66], one often designs boundary conditions to meet the electroneutrality condition

$$\sum_{s=1}^{n} z_s l_s = \sum_{s=1}^{n} z_s r_s = 0.$$

(1.5)

The electrochemical potential $\bar{\mu}_k(x) = \bar{\mu}_k^{id}(x) + \bar{\mu}_k^{ex}(x)$ for the k th ion species consists of the ideal component $\bar{\mu}_k^{id}(x)$ given by

$$\bar{\mu}_k^{id}(x) = z_k \phi(x) + \ln c_k(x), \tag{1.6}$$

and the excess component $\bar{\mu}_k^{ex}(x)$. The classical PNP model only deals with the ideal component $\bar{\mu}_k^{id}$, reflecting the collision between ion particles and water molecules and ignoring the size of ions. The excess electrochemical potential $\bar{\mu}_k^{ex}$ accounts for the finite size effect of ions [8,18–20,28,32,35,36,42,49,50,53,56,58].

An important quantity for characterizing ion channel properties is the so-called I-V (current-voltage) relation defined as follows. For fixed l_k's and r_k's, a solution $(\phi, c_k, \bar{J}_k)$ of the BVP (1.3) and (1.4) will depend on the voltage V only, and the current $\mathcal{I}$, the flow rate of charges, is thus related to the voltage V given by

$$\mathcal{I} = \sum_{s=1}^{n} z_s \bar{J}_s(V). \tag{1.7}$$

1.2　Flux ratios for permanent charge effects on ionic fluxes

Recall the concept of flux ratio for permanent charge effects on ionic fluxes introduced in [41]. For fixed boundary conditions (V,L,R) where $L = (l_1,\dots,l_n)^T$ and $R = (r_1,\dots,r_n)^T$, let $\bar{J}_k(Q)$ be the flux of the k-th ion species associated with the permanent charge Q, then the flux ratio for the k-th ion species is

$$\lambda_k(Q) = \frac{\bar{J}_k(Q)}{\bar{J}_k(0)}. \tag{1.8}$$

Since the boundary conditions are fixed, $\bar{J}_k(Q)$ and $\bar{J}_k(0)$ have the same sign as that of $\bar{\mu}_k(0) - \bar{\mu}_k(1)$ (see, e.g., [17,41]), and hence $\lambda_k(Q) \geq 0$. Therefore, the permanent charge Q enhances the flux of the k-th ion species if $\lambda_k(Q) > 1$ and it inhibits the flux of the k-th ion species if $\lambda_k(Q) < 1$. Regardless the relative positions of $\lambda_i(Q)$ and $\lambda_j(Q)$ to 1, we say the permanent charge Q enhances the flux of i-th ion species more than that of j-th ion species if $\lambda_i(Q) > \lambda_j(Q)$, even if, say, $1 > \lambda_i(Q) > \lambda_j(Q)$.

From [33,41,57], we know that for $n=2$ or $n=3$, depending on the boundary conditions, either $\lambda_k(Q) \geq 1$ or $\lambda_k(Q) < 1$ may occur. In particular, it is known [33,41] that,

$$\text{For } n=2 \text{ with } z_1 > 0 > z_2, \text{ if } Q > 0, \text{ then } \lambda_1(Q) < \lambda_2(Q). \tag{1.9}$$

We comment that Q needs not to be piecewise constant and the property holds true for any given boundary conditions. On the other hand, it was shown in [57] for a case study that, for $n=3$ with $z_1 > z_2 > 0 > z_3$, if $Q \geq 0$, then, dependent on boundary conditions and channel geometry, each of the following rather surprising situations is possible: (i) $\lambda_2(Q) > \lambda_3(Q)$; (ii) $\lambda_1(Q) > \lambda_2(Q)$ and $\lambda_1(Q) > \lambda_3(Q)$ simultaneously; (iii) $\lambda_1(Q) + \lambda_2(Q) > 2\lambda_3(Q)$.

1.3   Setup of our case study

In this paper, we continue the study on flux ratios started in [57] to examine the effects of permanent charges on individual fluxes for three ion species.

We now recall the basic setup from [57]. Assume

(A1) Consider three ion species ($n=3$) with $z_1 > z_2 > 0 > z_3$;

(A2) A piecewise constant permanent charge $Q=Q(x)$ with one nonzero region; that is, for a partition $0=x_0 < x_1 < x_2 < x_3 = 1$ of $[0,1]$,

$$Q(x) = \begin{cases} Q_1=Q_3=0, & x \in (x_0,x_1) \cup (x_2,x_3), \\ Q_2, & x \in (x_1,x_2), \end{cases} \tag{1.10}$$

where $|Q_2|$ is a constant small relative to l_k's and r_k's;

(A3) The electrochemical potential is ideal, that is $\bar{\mu}_k = \bar{\mu}_k^{id}$ given by (1.6);

(A4) Assume that $\bar{\varepsilon}_r(x)=1$ and $D_k(x)=D_k$ for some positive constants D_k.

In the following, we will assume $\varepsilon > 0$ small and treat system (1.3) as a singularly perturbed system. Then, we apply the GSP framework from [16,40] to the BVP (1.3) and (1.4). The following quantities α_j's for the channel geometry are crucial

$$\alpha_j = \frac{H(x_j)}{H(1)} \text{ where } x_j's \text{ are the jump points of } Q(x) \text{ and } H(x) = \int_0^x \frac{\mathrm{d}s}{h(s)}.$$

2   Reviews of relevant results

We will make two reviews that are directly relevant to the present work. The first is a brief review of the geometric singular perturbation (GSP) framework for PNP models developed in [16,40,44], etc. In particular, we will recall the meromorphic function whose roots are the starting point and several critical quantities for our study of the BVP. In the second part, we review relevant results from [57] on flux ratios with the setup in this paper for a case study. It is the new phenomena founded in [57] that motivate the further case study in this work. Some of the general results in [57] are also needed for the study in this paper.

2.1   Relevant results from GSP for PNP

We will give a brief and quick account of the GSP framework and relevant results in [16, 40, 44] (with slightly different notations) and refer the readers to these papers and references therein for details.

Denote the derivative with respect to x by overdot and introduce $u = \varepsilon\dot{\phi}$, $w = x$ and $J_k = \bar{J}_k / D_k$. System (1.3) becomes, for $k = 1,\ldots,n$,

$$\varepsilon\dot{\phi} = u, \quad \varepsilon\dot{u} = -\sum_{s=1}^{n} z_s c_s - Q(w) - \varepsilon\frac{h_w(w)}{h(w)}u,$$
$$\varepsilon\dot{c}_k = -z_k c_k u - \frac{\varepsilon}{h(w)}J_k, \quad \dot{J}_k = 0, \quad \dot{w} = 1. \tag{2.1}$$

The boundary condition (1.4) becomes, for $k = 1,\ldots,n$,

$$\phi(0) = V, \quad c_k(0) = l_k, \quad w(0) = 0; \qquad \phi(1) = 0, \quad c_k(1) = r_k, \quad w(1) = 1.$$

The boundary value problem (BVP) (1.3) and (1.4) can be converted to a connecting orbit problem: finding an orbit of (2.1) from B_L to B_R where

$$B_L = \{(\phi,u,C,J,w): \phi = V, \; C = L, \; w = 0\},$$
$$B_R = \{(\phi,u,C,J,w): \phi = 0, \; C = R, \; w = 1\}, \tag{2.2}$$

with $C = (c_1,\ldots,c_n)^T$, $J = (J_1,\ldots,J_n)^T$, $L = (l_1,\ldots,l_n)^T$ and $R = (r_1,\ldots,r_n)^T$.

Due to the jumps of $Q(x)$ in (1.10) at x_1 and x_2, it is convenient to preassign (unknown) values of ϕ and c_k's at each jump point x_j as

$$\phi(x_j) = \phi^{[j]}, \quad c_k(x_j) = c_k^{[j]}, \qquad j = 1,2. \tag{2.3}$$

We comment that, once these quantities are determined, so is a singular orbit ($\varepsilon = 0$) of the BVP (1.3) and (1.4) (see [16,40]).

The GSP developed in [16,40,44], etc. for PNP allows one to construct three singular orbits, one over each subinterval $[x_j, x_{j+1}]$ for $j = 0,1,2$ in terms of the preassigned values in (2.3). Each of the three orbits contains two "boundary layers" at the end points x_j and x_{j+1}, and one regular layers over the interval (x_j, x_{j+1}). One then matches these three orbits at x_1 and x_2 to obtain a governing system for the preassigned values in (2.3). In particular, one has

Proposition 2.1 (Theorem 3.1, [44]). *Let*

$$D = \Gamma - I^{-1}Jb^T, \tag{2.4}$$

where $\Gamma = diag\{z_1,\ldots,z_n\}$ is the diagonal matrix with z_k's on the diagonal, $I = \sum_{s=1}^{n} z_s J_s$, and $b = (z_1^2,\ldots,z_n^2)^T$. Let $\sigma_1,\ldots,\sigma_p$ be the distinct eigenvalues of D with algebraic multiplicities $s_1,\ldots,s_p$ so that $s_1 + \cdots + s_p = n$. (Note that 0 is always an eigenvalue and we choose $\sigma_p = 0$.) Then, for $j = 1,2,3$, the flux over the j-th interval is $J_k^{[j]} = I^{[j]}f_k^{[j]}$ where

$$I^{[j]} = \frac{V_j}{H(x_j) - H(x_{j-1})}\int_0^1 b^T e^{V_j Dz} C^{[j-1,+]} dz,$$
$$f_k^{[j]} = \frac{1}{z_k^2}\frac{\prod_{i=1}^{p}(z_k - \sigma_i)^{s_i}}{\prod_{1 \le i \le n, i \ne k}(z_k - \sigma_i)} \qquad for \; k = 1,\ldots,n. \tag{2.5}$$

For $n=3$, the governing system for the preassigned unknowns $(\phi^{[j]}, c_k^{[j]})$ for $j=1,2$ and $k=1,2,3$ in (2.3) is

$$\text{Matching at } x_1: \sum_{s=1}^{3} c_s^{[1,-]} = \sum_{s=1}^{3} c_s^{[1,+]} + Q_2(\phi^{[1]} - \phi^{[1,+]}), \quad J_k^{[1]} = J_k^{[2]},$$

$$\text{Matching at } x_2: \sum_{s=1}^{3} c_s^{[2,+]} = \sum_{s=1}^{3} c_s^{[2,-]} + Q_2(\phi^{[2]} - \phi^{[2,-]}), \quad J_k^{[2]} = J_k^{[3]}, \tag{2.6}$$

where $J_k^{[j]}$'s are provided in Proposition 2.1 and where, in terms of $(\phi^{[j]}, c_k^{[j]})$ variables, $\phi^{[j,+]}$ and $\phi^{[j,-]}$ are determined by

$$\sum_{s=1}^{3} z_s c_s^{[j]} e^{z_s(\phi^{[j]} - \phi^{[j,+]})} + Q_{j+1} = 0, \qquad \sum_{s=1}^{3} z_s c_s^{[j]} e^{z_s(\phi^{[j]} - \phi^{[j,-]})} + Q_j = 0,$$

and $c_k^{[j,+]}$ and $c_k^{[j,-]}$ are, in turn, given by

$$c_k^{[j,+]} = c_k^{[j]} e^{z_k(\phi^{[j]} - \phi^{[j,+]})}, \qquad c_k^{[j,-]} = c_k^{[j]} e^{z_k(\phi^{[j]} - \phi^{[j,-]})}.$$

2.2 Relevant results for small Q and $n=3$ from [57]

In [57], for three ion species with valences $z_1 > z_2 > 0 > z_3$ and for small $|Q_2|$, a systematic investigation on comparative effects of permanent charge Q was initiated and a rich set of phenomena was revealed, much more beyond the case with two ion species done in [33, 41]. Even though the study in [57] was focused on special cases, many findings were quite counterintuitive. We will review the framework set in [57] and some relevant results in this part.

2.2.1 Comparative effects of permanent charge Q with small $|Q_2|$

In [57] and this paper, the main focus is to study the effects of small permanent charges on individual fluxes and we are mainly interested in properties based on J_k up to $O(Q_2)$.

For small Q_2, we expand the quantities $(\phi^{[j]}, c_k^{[j]})$ in (2.3) as follows

$$\phi^{[j]} = \phi_0^{[j]} + \phi_1^{[j]} Q_2 + O(Q_2^2), \quad c_k^{[j]} = c_{k0}^{[j]} + c_{k1}^{[j]} Q_2 + O(Q_2^2), \quad J_k = J_{k0} + J_{k1} Q_2 + O(Q_2^2). \tag{2.7}$$

With expansions in (2.7), the flux ratio $\lambda_k(Q)$ of the k-th ion species in (1.8) and the flux ratio difference $\lambda_i(Q) - \lambda_j(Q)$ between the i-th and the j-th ion species are

$$\lambda_k(Q) = \frac{J_k(Q)}{J_k(0)} = 1 + \tau_k Q_2 + o(Q_2), \quad \lambda_i(Q) - \lambda_j(Q) = \tau_{ij} Q_2 + o(Q_2), \tag{2.8}$$

where, from (2.7),

$$\tau_k = \frac{J_{k1}}{J_{k0}} \quad \text{and} \quad \tau_{ij} = \tau_i - \tau_j. \tag{2.9}$$

Therefore, comparative effects of small Q on fluxes J_i and J_j are reduced to the study of signs of τ_{ij}, which are determined by boundary conditions (V, L, R) and channel geometry characters (α_1, α_2).

We will use the following notations for simplicity.

$$
\begin{aligned}
S_L &= \sum_{s=1}^{3} l_s, \quad S_R = \sum_{s=1}^{3} r_s, \quad \Lambda_L = \sum_{s=1}^{3} z_s^2 l_s, \quad \Lambda_R = \sum_{s=1}^{3} z_s^2 r_s, \\
m_l &= -z_1 z_2 z_3 \frac{S_L}{\Lambda_L}, \quad m_r = -z_1 z_2 z_3 \frac{S_R}{\Lambda_R}, \quad \rho = \frac{\Lambda_R}{\Lambda_L}.
\end{aligned}
\tag{2.10}
$$

Let D_0 be the zeroth order of D in Q_2. For $V \neq 0$, under the boundary electroneutrality conditions, let $g : \mathbb{C} \to \mathbb{C}$ be the meromorphic function defined as

$$
g(\sigma) := \sum_{s=1}^{3} \frac{z_s^2 r_s}{z_s - \sigma} - e^{V\sigma} \sum_{s=1}^{3} \frac{z_s^2 l_s}{z_s - \sigma},
\tag{2.11}
$$

and denote

$$
\gamma(\sigma) = g(\sigma) \frac{1}{\sigma} \prod_{s=1}^{3} (\sigma - z_s) = e^{\sigma V} L(\sigma) - R(\sigma),
\tag{2.12}
$$

where

$$
L(\sigma) = z_1 z_2 z_3 S_L + \sigma \Lambda_L = \Lambda_L(\sigma - m_l), \quad R(\sigma) = z_1 z_2 z_3 S_R + \sigma \Lambda_R = \Lambda_R(\sigma - m_r).
$$

As a direct consequence of a general result in [44], one has that D_0 has a zero eigenvalue and its nonzero eigenvalues σ_{10} and σ_{20} are the unique solutions of $\gamma(\sigma) = 0$ in the stripe

$$
S = \left\{ z \in \mathbb{C} : \operatorname{Im}(z) \in (-\pi/|V|, \pi/|V|) \right\}.
$$

We now recall several results from [57] that will be used in this work.

Proposition 2.2 (Proposition 6.3, [57])**.** *Suppose $V \neq 0$.*

(i) If $\sigma_{10} \sigma_{20} \neq 0$, then $\phi_0^{[j]}$ is uniquely determined by

$$
e_0^T e^{(V - \phi_0^{[j]}) D_0} L - S_L = \alpha_j g'(0).
\tag{2.13}
$$

(ii) If $\sigma_{10} \neq 0$ and $\sigma_{20} = 0$, then $\phi_0^{[j]}$ is uniquely determined by

$$
e_0^T \Gamma^{-1} e^{(V - \phi_0^{[j]}) D_0} - \sum_{s=1}^{3} \frac{l_s}{z_s} - (V - \phi_0^{[j]}) S_L = \alpha_j g''(0).
$$

Proposition 2.3 (Proposition 3.3, [57]). *One has*

$$\tau_{ij} = T_{ij}(\phi_0^{[2]}) - T_{ij}(\phi_0^{[1]})$$

where, for a permutation $\{i,j,k\}$ of $\{1,2,3\}$ (the convention to be used in the rest),

(i) *if $\sigma_{10} \neq \sigma_{20}$, then*

$$T_{ij}(\phi) = \frac{(z_i - z_j)(\sigma_{10} - z_k)}{\sigma_{10}\gamma'(\sigma_{10})}(e^{\sigma_{10}\phi} - 1) + \frac{(z_i - z_j)(\sigma_{20} - z_k)}{\sigma_{20}\gamma'(\sigma_{20})}(e^{\sigma_{20}\phi} - 1); \qquad (2.14)$$

(If $\sigma_{j0} = 0$, then the above formula is defined by applying the L'Hopital rule.)

(ii) *if $\sigma_{10} = \sigma_{20} = \sigma_0$, then*

$$T_{ij}(\phi) = \frac{2(z_i - z_j)(\sigma_0 - z_k)}{\sigma_0\gamma''(\sigma_0)}\Big(\phi e^{\sigma_0\phi} - (e^{\sigma_0\phi} - 1)\big(\frac{\gamma'''(\sigma_0)}{3\gamma''(\sigma_0)} + \frac{1}{\sigma_0} + \frac{1}{z_k - \sigma_0}\big)\Big).$$

(If $\sigma_0 = 0$, then the above formula is defined by applying the L'Hopital rule.)

We recall that, if $V = 0$, then $\phi_0^{[1]} = \phi_0^{[2]} = 0$ (Proposition 2.1 in [17]), and hence, $\tau_{ij} = 0$. Also if $V > 0$ (resp. $V < 0$), then $\phi'(x) < 0$ and $\phi_0^{[1]} > \phi_0^{[2]}$ (resp. $\phi'(x) > 0$ and $\phi_0^{[1]} < \phi_0^{[2]}$). In the sequel, we will assume $V \neq 0$ Therefore, for $\sigma_{10}, \sigma_{20} \in \mathbb{R}$, the domain of $T_{ij}(\phi)$ is $\mathbb{R}\backslash\{0\}$; for $\sigma_{10} = \overline{\sigma_{20}} = x + iy$ with $y \neq 0$, the domain of $T_{ij}(\phi)$ is $(-\pi/|y|, 0) \cup (0, \pi/|y|)$.

Remark 2.1. (i) It follows from Proposition 3.5 in [57] that for $V \neq 0$, the situation $\tau_{12} = \tau_{23} = \tau_{13} = 0$ cannot occur.

(ii) For a fixed boundary condition, $\phi_0^{[j]}$ depends on α_j, so we will use $\tau_{ij}(\alpha_1, \alpha_2)$ whenever needed to emphasize the dependence of τ_{ij} on $(\alpha_1, \alpha_2) \in \Delta$, where

$$\Delta := \{(\alpha_1, \alpha_2) \,|\, 0 \leq \alpha_1 \leq \alpha_2 \leq 1\}.$$

3 New case study on τ_{ij} for $\sigma_{10} = \overline{\sigma_{20}} = x + iy$

In [57], the authors presented preliminary results for $\sigma_{10} \neq \sigma_{20} \in \mathbb{R}$ and $\sigma_{10} = \sigma_{20} \in \mathbb{R}$ and applied to study the equi-chemical-potential-difference case. Here we give some preliminary results for $\sigma_{10} = \overline{\sigma_{20}} \in \mathbb{C}$.

3.1 Critical points of $T_{ij}(\phi)$, the quantity θ_{ij} and the function $P_{ij}(\alpha)$

In this case, the function $T_{ij}(\phi)$ in (2.14) is still real-value and we will make a preparation before a statement of the result. By Proposition 2.1, we know $y \in (-\pi/|V|, \pi/|V|)$. For $\sigma_{10} = \overline{\sigma_{20}} = x + iy$, one has, from (2.12),

$$e^{(x+iy)V} = \frac{\Lambda_R}{\Lambda_L}\frac{x - m_r + iy}{x - m_l + iy},$$

which leads to

$$e^{xV}\cos(yV)=\rho\frac{y^2+(x-m_l)(x-m_r)}{y^2+(x-m_l)^2} \quad \text{and} \quad e^{xV}\sin(yV)=\rho\frac{y(m_r-m_l)}{y^2+(x-m_l)^2}. \tag{3.1}$$

Thus,

$$e^{2xV}=\rho^2\frac{y^2+(x-m_r)^2}{y^2+(x-m_l)^2}, \quad \text{and hence,} \quad y^2=\frac{\rho^2(x-m_r)^2-e^{2xV}(x-m_l)^2}{e^{2xV}-\rho^2}.$$

Lemma 3.1. *If $\sigma_{10}=\overline{\sigma_{20}}=x+iy$ with $y\neq0$, then $V(m_r-m_l)>0$.*

Proof. It is a consequence of the 2nd equation in (3.1) and $yV\sin(yV)>0$. □

It follows from (2.12) that $\gamma'(x+iy)=\zeta+i\kappa$ where

$$\begin{aligned}
\zeta&=\Lambda_R\frac{(m_l-x)(m_r-m_l)+V(x-m_r)(y^2+(x-m_l)^2)}{y^2+(x-m_l)^2}, \\
\kappa&=\Lambda_R\frac{y(m_r-m_l)+yV(y^2+(x-m_l)^2)}{y^2+(x-m_l)^2}.
\end{aligned} \tag{3.2}$$

Lemma 3.2. *Assume $\sigma_{10}=\overline{\sigma_{20}}=x+iy$ with $y\neq0$. Over $(-\pi/|y|,\pi/|y|)$, one has*

(i) if $y\kappa+(x-z_k)\zeta=0$, then $\phi=0$ is the unique critical point of $T_{ij}(\phi)$;

(ii) if $y\kappa+(x-z_k)\zeta\neq0$, then $T_{ij}(\phi)$ has two critical points, one in $(-\frac{\pi}{|y|},0)$ and the other in $(0,\frac{\pi}{|y|})$.

Proof. It follows from (2.14) that

$$T'_{ij}(\phi)=2(z_i-z_j)e^{x\phi}\frac{\cos(y\phi)(y\kappa+(x-z_k)\zeta)-\sin(y\phi)(y\zeta-(x-z_k)\kappa)}{\zeta^2+\kappa^2}.$$

(i) If $y\kappa+(x-z_k)\zeta=0$, then $\zeta\neq0$ since, otherwise, $\kappa=0$ too that contradicts to $\zeta+i\kappa\neq0$. One then gets

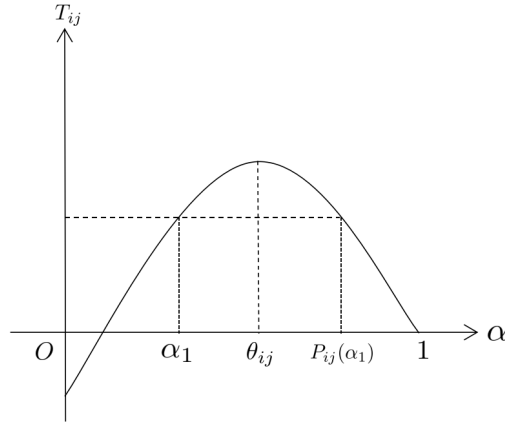$$T'_{ij}(\phi)=-2(z_i-z_j)e^{x\phi}\sin(y\phi)\frac{y}{\zeta}. \tag{3.3}$$

Thus $T'_{ij}(\phi)=0$ has a unique root $\phi=0$.

(ii) If $y\kappa+(x-z_k)\zeta\neq0$, then $T'_{ij}(\phi)=0$ implies $\sin(y\phi)\neq0$, and hence,

$$\cot(y\phi)=\frac{y\zeta-(x-z_k)\kappa}{y\kappa+(x-z_k)\zeta},$$

which has two roots in $(-\frac{\pi}{|y|},\frac{\pi}{|y|})$, one in $(-\frac{\pi}{|y|},0)$ and the other in $(0,\frac{\pi}{|y|})$. □

Figure 1: Function $P_{ij}(\alpha)$ from $T_{ij}(\alpha)$

For $y\kappa+(x-z_k)\zeta\neq0$, we denote the two critical points of $T_{ij}(\phi)$ in $(-\pi/|y|,\pi/|y|)$ by V_{ij} and $\tilde{V}_{ij}$, and set

$$\theta_{ij}=\frac{1}{g'(0)}e_0^T\left(e^{(V-V_{ij})D_0}L-L\right)\quad\text{and}\quad\tilde{\theta}_{ij}=\frac{1}{g'(0)}e_0^T\left(e^{(V-\tilde{V}_{ij})D_0}L-L\right).$$

Without loss of generality, we assume $V\tilde{V}_{ij}<0<VV_{ij}$.

Proposition 3.1. *If $V>0$ (resp. $V<0$), then θ_{ij} and $\tilde{\theta}_{ij}$ are decreasing (resp. increasing) in V_{ij} and $\tilde{V}_{ij}$, respectively. Furthermore, $\theta_{ij}<1<\tilde{\theta}_{ij}$ holds true, and one has $\theta_{ij}\in[0,1]$ if and only if V_{ij} lies between 0 and V.*

When $\theta_{ij}\in[0,1]$, we can define a function $P_{ij}:(-\infty,\theta_{ij}]\rightarrow[\theta_{ij},\infty)$ as follows: $P_{ij}(\alpha)=\beta$ if $T_{ij}(\beta)=T_{ij}(\alpha)$ (see Fig. 1). This function plays an important role in characterizing transitions from one behavior of permanent charge effect to another.

3.2   Signs of τ_{ij}

In this section, we will discuss signs of τ_{ij} for $\sigma_{10}=\overline{\sigma_{20}}=x+iy$ with $y\neq0$, especially the case with $x=0$.

3.2.1   General results

The following result gives the conditions of determining signs of τ_{ij}, which are determined by (V,L,R) and (α_1,α_2). As in Remark 2.1, we will use $\tau_{ij}(\alpha_1,\alpha_2)$ whenever needed to emphasize the dependence of τ_{ij} on $(\alpha_1,\alpha_2)\in\Delta$.

Proposition 3.2. *Assume $\sigma_{10}=\overline{\sigma_{20}}=x+iy$ with $y\neq0$. For $V\neq0$, one has*

(i)   if $y\kappa+(x-z_k)\zeta=0$, then $(z_i-z_j)\tau_{ij}(\alpha_1,\alpha_2)\zeta>0$ for any $(\alpha_1,\alpha_2)\in\Delta$;

    (ii) if $y\kappa+(x-z_k)\zeta\neq0$ and $\theta_{ij}\in[0,1]$, then exactly one of the followings occurs

        (a) when $(z_i-z_j)V(y\kappa+(x-z_k)\zeta)<0$,

$$\tau_{ij}(\alpha_1,\alpha_2)=\begin{cases} <0, & \alpha_1<\theta_{ij} \quad and \quad \alpha_2<P_{ij}(\alpha_1),\\ >0, & \alpha_1>\theta_{ij} \quad or \quad \alpha_2>P_{ij}(\alpha_1); \end{cases}$$

        (b) when $(z_i-z_j)V(y\kappa+(x-z_k)\zeta)>0$,

$$\tau_{ij}(\alpha_1,\alpha_2)=\begin{cases} >0, & \alpha_1<\theta_{ij} \quad and \quad \alpha_2<P_{ij}(\alpha_1),\\ <0, & \alpha_1>\theta_{ij} \quad or \quad \alpha_2>P_{ij}(\alpha_1). \end{cases}$$

Proof. For $V\neq0$, it can be shown that $\tau_{ij}(\alpha,\alpha)=0$ for any $\alpha\in[0,1]$ and

$$\partial_{\alpha_1}\tau_{ij}(\alpha_1,\alpha_2)=-\frac{\mathrm{d}\phi_0^{[1]}}{\mathrm{d}\alpha_1}T'_{ij}(\phi_0^{[1]}), \qquad \partial_{\alpha_2}\tau_{ij}(\alpha_1,\alpha_2)=\frac{\mathrm{d}\phi_0^{[2]}}{\mathrm{d}\alpha_2}T'_{ij}(\phi_0^{[2]}). \tag{3.4}$$

Note that for $V>0$, $\frac{\mathrm{d}\phi_0^{[1]}}{\mathrm{d}\alpha_1},\frac{\mathrm{d}\phi_0^{[2]}}{\mathrm{d}\alpha_2}<0$; for $V<0$, $\frac{\mathrm{d}\phi_0^{[1]}}{\mathrm{d}\alpha_1},\frac{\mathrm{d}\phi_0^{[2]}}{\mathrm{d}\alpha_2}>0$.
    (i) Suppose $y\kappa+(x-z_k)\zeta=0$. Since $y\phi\in(-\pi,\pi)$, one has $y\phi\sin(y\phi)>0$ if $\phi\neq0$. It then follows from (3.3) that

$$(z_i-z_j)\zeta\phi T'_{ij}(\phi)<0 \qquad \text{for } \phi\neq0. \tag{3.5}$$

Recall that $\tau_{ij}=T_{ij}(\phi_0^{[2]})-T_{ij}(\phi_0^{[1]})$. Thus, for some ϕ^* between $\phi_0^{[1]}$ and $\phi_0^{[2]}$,

$$(z_i-z_j)\zeta\phi^*\tau_{ij}=(z_i-z_j)\zeta\phi^*T'_{ij}(\phi^*)(\phi_0^{[2]}-\phi_0^{[1]}). \tag{3.6}$$

For $V>0$, one has $\phi_0^{[1]}>\phi_0^{[2]}>0$, and hence, $\phi^*>0$. It then follows from (3.5) and (3.6) that $(z_i-z_j)\zeta\tau_{ij}>0$. Similarly, for $V<0$, one also has $(z_i-z_j)\zeta\tau_{ij}>0$.

    (ii) Suppose that $y\kappa+(x-z_k)\zeta\neq0$ and $\theta_{ij}\in[0,1]$. For ease of the proof, we set

$$V_{ij}^1=V_{ij}, \quad V_{ij}^2=\tilde{V}_{ij}, \quad \theta_{ij}^1=\theta_{ij}, \quad \theta_{ij}^2=\tilde{\theta}_{ij}.$$

Note that $0\leq\theta_{ij}^1\leq1<\theta_{ij}^2$. Since $T'_{ij}(V_{ij}^s)=0$, $s=1,2$, a direct calculation gives

$$\partial_{\alpha_1\alpha_1}\tau_{ij}(\theta_{ij}^s,\theta_{ij}^s)=-\left(\frac{\mathrm{d}\phi_0^{[1]}}{\mathrm{d}\alpha_1}\right)^2 T''_{ij}(V_{ij}^s), \quad \partial_{\alpha_2\alpha_2}\tau_{ij}(\theta_{ij}^s,\theta_{ij}^s)=\left(\frac{\mathrm{d}\phi_0^{[2]}}{\mathrm{d}\alpha_2}\right)^2 T''_{ij}(V_{ij}^s),$$

where

$$T''_{ij}(V_{ij}^s)=-\frac{2(z_i-z_j)y\sin(yV_{ij}^s)e^{xV_{ij}^s}}{\zeta^2+\kappa^2}\frac{(y\kappa+(x-z_k)\zeta)^2+(y\zeta-(x-z_k)\kappa)^2}{y\kappa+(x-z_k)\zeta}.$$

By
$$yV_{ij}^1 \in (-\pi,\pi), \quad yV_{ij}^2 \in (-\pi,\pi), \qquad V_{ij}^1 V_{ij}^2 < 0$$
one has $\sin(yV_{ij}^1)\sin(yV_{ij}^2)<0$, which leads to $T_{ij}''(V_{ij}^1)T_{ij}''(V_{ij}^2)<0$. It follows from
$$\partial_{\alpha_1\alpha_1}\tau_{ij}(\theta_{ij}^s,\theta_{ij}^s)\partial_{\alpha_2\alpha_2}\tau_{ij}(\theta_{ij}^s,\theta_{ij}^s)<0, \quad \partial_{\alpha_1\alpha_2}\tau_{ij}(\alpha_1,\alpha_2)=\partial_{\alpha_2\alpha_1}\tau_{ij}(\alpha_1,\alpha_2)=0$$
that $(\theta_{ij}^1,\theta_{ij}^1)\in\Delta$ and $(\theta_{ij}^2,\theta_{ij}^2)\notin\Delta$ are two saddle points of $\tau_{ij}(\alpha_1,\alpha_2)$.

When $(z_i-z_j)V(y\kappa+(x-z_k)\zeta)<0$, one has $T_{ij}''(V_{ij}^1)>0>T_{ij}''(V_{ij}^2)$. For any $\tilde{\alpha}_1<\tilde{\alpha}_2\leq \theta_{ij}^1\leq\tilde{\beta}_1<\tilde{\beta}_2\leq\theta_{ij}^2\leq\tilde{\eta}_1<\tilde{\eta}_2$, it follows from
$$\partial_{\alpha_1\alpha_1}\tau_{ij}(\theta_{ij}^1,\theta_{ij}^1)<0<\partial_{\alpha_2\alpha_2}\tau_{ij}(\theta_{ij}^1,\theta_{ij}^1), \quad \partial_{\alpha_1\alpha_1}\tau_{ij}(\theta_{ij}^2,\theta_{ij}^2)>0>\partial_{\alpha_2\alpha_2}\tau_{ij}(\theta_{ij}^2,\theta_{ij}^2)$$
that
$$\partial_{\alpha_1}\tau_{ij}(\tilde{\alpha}_1,\tilde{\alpha}_2)>0, \quad \partial_{\alpha_1}\tau_{ij}(\tilde{\beta}_1,\tilde{\beta}_2)<0<\partial_{\alpha_2}\tau_{ij}(\tilde{\beta}_1,\tilde{\beta}_2), \quad \partial_{\alpha_2}\tau_{ij}(\tilde{\eta}_1,\tilde{\eta}_2)<0.$$
Thus,
$$\tau_{ij}(\tilde{\alpha}_1,\tilde{\alpha}_2)<0<\tau_{ij}(\tilde{\beta}_1,\tilde{\beta}_2), \quad \tau_{ij}(\tilde{\eta}_1,\tilde{\eta}_2)<0.$$
Similarly, when $(z_i-z_j)V(y\kappa+(x-z_k)\zeta)>0$, one has
$$\tau_{ij}(\tilde{\alpha}_1,\tilde{\alpha}_2)>0>\tau_{ij}(\tilde{\beta}_1,\tilde{\beta}_2), \quad \tau_{ij}(\tilde{\eta}_1,\tilde{\eta}_2)>0.$$

Moreover, it follows from the implicit function theorem that $\tau_{ij}(\alpha_1,\alpha_2)=0$ has a solution $\alpha_2=P_{ij}(\alpha_1)\geq\theta_{ij}^1$ for $\alpha_1\in[0,\theta_{ij}^1]$ satisfying $\theta_{ij}^1=P_{ij}(\theta_{ij}^1)$ (see Fig. 1). The proof is completed. $\square$

3.2.2 Special case with $\sigma_{10}=\overline{\sigma_{20}}=iy$ with $y>0$

In this part, we will conduct a detailed study for the case with $\sigma_{10}=\overline{\sigma_{20}}=iy$ with $y>0$, more precisely, $0<y<\pi/|V|$. It follows from (3.1) that
$$\cos(yV)=\rho\frac{y^2+m_l m_r}{y^2+m_l^2} \quad \text{and} \quad \sin(yV)=\rho\frac{y(m_r-m_l)}{y^2+m_l^2}. \tag{3.7}$$

By the symmetry in Remark 1.1 and Lemma 3.1, we only consider $m_l<m_r$, or equivalently, $V>0$. It is direct to obtain from $yV\in(0,\pi)$ and (3.7) that $yV\in(0,\frac{\pi}{2})$.

Lemma 3.3. *Assume $m_l<m_r$. $\sigma_{10}=\overline{\sigma_{20}}=iy$ with $y>0$ is the solution of $\gamma(\sigma)=0$ if and only if*
$$V=\frac{1}{y}\cot^{-1}\left(\frac{\rho^2 m_r+m_l}{\sqrt{(\rho^2 m_r^2-m_l^2)(1-\rho^2)}}\right)\in(0,\frac{\pi}{2y}), \tag{3.8}$$
where
$$y=\sqrt{\frac{\rho^2 m_r^2-m_l^2}{1-\rho^2}} \quad \text{and} \quad \rho\in(\frac{m_l}{m_r},1).$$

Proof. By (3.7), one has

$$\rho^2 \frac{(y^2+m_l m_r)^2+y^2(m_r-m_l)^2}{(y^2+m_l^2)^2}=1 \implies \rho^2(y^2+m_r^2)=y^2+m_l^2 \implies y^2=\frac{\rho^2 m_r^2-m_l^2}{1-\rho^2}.$$

It is easy to see that the right-hand side is positive if and only if $m_l/m_r<\rho<1$ which, in turn, is equivalent to $S_L<S_R$ and $\Lambda_R<\Lambda_L$. The formula (3.8) follows from

$$y=\sqrt{\frac{\rho^2 m_r^2-m_l^2}{1-\rho^2}}>0 \quad \text{and} \quad \cot(yV)=\frac{y^2+m_l m_r}{y(m_r-m_l)}=\frac{\rho^2 m_r+m_l}{\sqrt{(\rho^2 m_r^2-m_l^2)(1-\rho^2)}}>0.$$

The proof is completed. $\qquad\square$

By (3.2) and $\sigma_{10}=\overline{\sigma_{20}}=iy$, one has

$$\zeta=\Lambda_R\frac{m_l(m_r-m_l)-m_r V(y^2+m_l^2)}{y^2+m_l^2}, \quad \kappa=\Lambda_R\frac{y(m_r-m_l)+yV(y^2+m_l^2)}{y^2+m_l^2}. \qquad (3.9)$$

Let

$$V_0=\frac{m_l(m_r-m_l)}{m_r(y^2+m_l^2)}.$$

Lemma 3.4. *Assume $m_l<m_r$ and $\sigma_{10}=\overline{\sigma_{20}}=iy$ with $y>0$. One has*

$$V>V_0, \quad \kappa>0>\zeta, \quad y\zeta+m_r\kappa>0.$$

Proof. It follows from $yV\in(0,\frac{\pi}{2})$ and $\rho\in(\frac{m_l}{m_r},1)$ that

$$yV_0-yV=\frac{m_l\sin(yV)}{m_r\rho}-yV<\sin(yV)-yV<0,$$

and hence $V>V_0$ by $y>0$. It is direct to obtain from $m_l<m_r$ and (3.9) that $\kappa>0$, and $\zeta<0$ by $V>V_0$. Note that

$$\frac{\zeta}{\kappa}=\frac{m_l(m_r-m_l)-m_r V(y^2+m_l^2)}{y(m_r-m_l)+yV(y^2+m_l^2)}<0.$$

It can be shown from $V>0$ that $\frac{\zeta}{\kappa}\in(-\frac{m_r}{y},0)$, which leads to $y\zeta+m_r\kappa>0$. The proof is completed. $\qquad\square$

For $y\kappa-z_k\zeta\neq0$, let

$$\theta_{ij}=\frac{1}{g'(0)}e_0^T\left(e^{(V-V_{ij})D_0}L-L\right), \quad V_{ij}=\frac{1}{y}\cot^{-1}\left(\frac{y\zeta+z_k\kappa}{y\kappa-z_k\zeta}\right)\in(0,\frac{\pi}{y}). \qquad (3.10)$$

One has from Proposition 3.1 that $\theta_{ij} < 1$. In the following, we will determine conditions for $\theta_{ij} > 0$.

It follows from Proposition 3.1, $yV \in (0, \frac{\pi}{2})$ and $yV_{ij} \in (0, \pi)$ that $\theta_{ij} > 0$ if and only if $V_{ij} < V$ if and only if $\cot(yV) < \cot(yV_{ij})$. Since $\cot(yV) > 0$, we first determine conditions for $\cot(yV_{ij}) > 0$, or equivalently, for $(y\zeta + z_k\kappa)(y\kappa - z_k\zeta) > 0$. Note that $z_3 < 0 < z_2 < m_l < m_r < z_1$. One has from Lemma 3.4 that

$$y\kappa - z_1\zeta > y\kappa - z_2\zeta > 0, \quad y\zeta + z_1\kappa > 0 > y\zeta + z_3\kappa. \tag{3.11}$$

Lemma 3.5. *Assume $m_l < m_r$ and $\sigma_{10} = \overline{\sigma_{20}} = iy$ with $y > 0$. One has*
(i) $y\kappa - z_3\zeta < 0$ if and only if

$$y^2 + z_3 m_r < 0 \quad and \quad V > \frac{(z_3 m_l - y^2)(m_r - m_l)}{(z_3 m_r + y^2)(y^2 + m_l^2)}. \tag{3.12}$$

(ii) $y\zeta + z_2\kappa > 0$ if and only if

$$V < \frac{(m_l + z_2)(m_r - m_l)}{(m_r - z_2)(y^2 + m_l^2)}.$$

Proof. (i) Using (3.9), one has that $y\kappa - z_3\zeta < 0$ if and only if

$$(y^2 - z_3 m_l)(m_r - m_l) + V(y^2 + z_3 m_r)(y^2 + m_l^2) < 0.$$

If $y^2 + z_3 m_r \geq 0$, then the above fails since $z_3 < 0$, $V > 0$ and $m_l < m_r$. If $y^2 + z_3 m_r < 0$, then the above is equivalent to

$$V > \frac{(z_3 m_l - y^2)(m_r - m_l)}{(z_3 m_r + y^2)(y^2 + m_l^2)}.$$

(ii) Using (3.9), one has that $y\zeta + z_2\kappa > 0$ if and only if

$$y(m_l + z_2)(m_r - m_l) - Vy(m_r - z_2)(y^2 + m_l^2) > 0.$$

By $m_r > z_2$ and $y > 0$, the above is equivalent to

$$V < \frac{(m_l + z_2)(m_r - m_l)}{(m_r - z_2)(y^2 + m_l^2)}.$$

The proof is completed. $\qquad\square$

We now determine conditions for $\theta_{ij} > 0$, or equivalently, for the sign of $\cot(yV) - \cot(yV_{ij})$. It is direct to obtain

$$\cot(yV) - \cot(yV_{ij}) = \frac{M_{ij}(V - V_{ij}^*)(y^2 + m_l^2)}{y(y\kappa - z_k\zeta)(m_r - m_l)}, \tag{3.13}$$

where

$$M_{ij} = (z_k m_l + y^2)(y^2 + m_r^2) \quad and \quad V_{ij}^* = \frac{(z_k m_r - y^2)(m_r - m_l)}{M_{ij}}.$$

Lemma 3.6. *Assume $m_l < m_r$ and $\sigma_{10} = \overline{\sigma_{20}} = iy$ with $y > 0$. One has*

(i) *$\theta_{12} > 0$ if and only if $y\kappa - z_3\zeta < 0$ and $M_{12}(V - V_{12}^*) > 0$;*

(ii) *$\theta_{13} > 0$ if and only if $y\zeta + z_2\kappa > 0$ and $V < V_{13}^*$;*

(iii) *$\theta_{23} > 0$ if and only if $V < V_{23}^*$.*

Proof. It follows from Proposition 3.1, $yV \in (0, \frac{\pi}{2})$ and $yV_{ij} \in (0, \pi)$ that $\theta_{ij} > 0$ if and only if $V_{ij} < V$ if and only if $\cot(yV) < \cot(yV_{ij})$. Note that $\cot(yV) > 0$.

(i) Note that $y\zeta + z_3\kappa < 0$. If $y\kappa - z_3\zeta > 0$, then it follows from (3.10) that $\cot(yV_{12}) < 0$, which leads to $\theta_{12} < 0$. If $y\kappa - z_3\zeta < 0$, then it follows from (3.13) that $\cot(yV) < \cot(yV_{12})$ if and only if $M_{12}(V - V_{12}^*) > 0$.

(ii) Note that $y\kappa - z_2\zeta > 0$. If $y\zeta + z_2\kappa < 0$, then it follows from (3.10) that $\cot(yV_{13}) < 0$, which leads to $\theta_{13} < 0$. If $y\zeta + z_2\kappa > 0$, then it follows from (3.13) and $M_{13} > 0$ that $\cot(yV) < \cot(yV_{13})$ if and only if $V < V_{13}^*$.

(iii) Note that $y\kappa - z_1\zeta > 0$ and $y\zeta + z_1\kappa > 0$. It follows from (3.13) and $M_{23} > 0$ that $\cot(yV) < \cot(yV_{23})$ if and only if $V < V_{23}^*$. The proof is completed. $\square$

Remark 3.1. (i) Note that $y^2 + z_3m_r < y^2 + z_3m_l$ and

$$V_{12}^* - \frac{(z_3m_l - y^2)(m_r - m_l)}{(z_3m_r + y^2)(y^2 + m_l^2)} = \frac{y^2(y^2 + z_3^2)(m_r + m_l)(m_r - m_l)^2}{(y^2 + z_3m_r)(y^2 + z_3m_l)(y^2 + m_r^2)(y^2 + m_l^2)}.$$

By (i) in Lemma 3.5 and (i) in Lemma 3.6, it can be shown that $\theta_{12} > 0$ if and only if either

$$y^2 + z_3m_r < y^2 + z_3m_l < 0 \quad \text{and} \quad V_{12}^* > V > \frac{(z_3m_l - y^2)(m_r - m_l)}{(z_3m_r + y^2)(y^2 + m_l^2)},$$

or

$$y^2 + z_3m_r < 0 < y^2 + z_3m_l \quad \text{and} \quad V > V_{12}^*.$$

(ii) Note that

$$V_{13}^* - \frac{(m_l + z_2)(m_r - m_l)}{(m_r - z_2)(y^2 + m_l^2)} = \frac{(y^2 + z_2^2)(y^2 + m_lm_r)(m_l^2 - m_r^2)}{(m_r - z_2)(y^2 + z_2m_l)(y^2 + m_r^2)(y^2 + m_l^2)} < 0.$$

By (ii) in Lemma 3.5, we can rewrite (ii) in Lemma 3.6 as $\theta_{13} > 0$ if and only if $V < V_{13}^*$.

The next result gives the order of θ_{12}, θ_{13} and θ_{23}.

Lemma 3.7. *Assume $m_l < m_r$ and $\sigma_{10} = \overline{\sigma_{20}} = iy$ with $y > 0$. If $y\kappa - z_3\zeta > 0$, then $\theta_{12} < \theta_{13} < \theta_{23}$; if $y\kappa - z_3\zeta < 0$, then $\theta_{13} < \theta_{23} < \theta_{12}$. In particular, $\theta_{13} < 0$.*

Proof. A direct calculation gives

$$\frac{y\zeta+z_i\kappa}{y\kappa-z_i\zeta}-\frac{y\zeta+z_j\kappa}{y\kappa-z_j\zeta}=\frac{y(z_i-z_j)(\kappa^2+\zeta^2)}{(y\kappa-z_i\zeta)(y\kappa-z_j\zeta)}.$$

Note that $y\kappa-z_1\zeta>y\kappa-z_2\zeta>0$. If $y\kappa-z_3\zeta>0$, then it is direct to obtain

$$\frac{y\zeta+z_1\kappa}{y\kappa-z_1\zeta}>\frac{y\zeta+z_2\kappa}{y\kappa-z_2\zeta}>\frac{y\zeta+z_3\kappa}{y\kappa-z_3\zeta},$$

which leads to $V_{12}>V_{13}>V_{23}$ by (3.10), and hence $\theta_{12}<\theta_{13}<\theta_{23}$. Similarly, one has that if $y\kappa-z_3\zeta<0$, then $\theta_{13}<\theta_{23}<\theta_{12}$.

Next, we prove $\theta_{13}<0$. If $y\zeta+z_2\kappa<0$, then one has from Lemma 3.6 that $\theta_{13}<0$. If $y\zeta+z_2\kappa>0$, then one has from $y\kappa-z_2\zeta>0$ and (3.10) that $\cot(yV_{13})>0$ and $yV_{13}\in(0,\frac{\pi}{2})$. Note that,

$$V_0-V_{13}^*=\frac{y^2(m_r^2-m_l^2)\big((m_l-z_2)m_r+y^2+z_2m_l\big)}{M_{13}m_r(y^2+m_l^2)}.$$

It follows from $m_r>m_l>z_2>0$, $M_{13}>0$ and Lemma 3.4 that $V>V_0>V_{13}^*$, which leads to $\theta_{13}<0$ by Lemma 3.6. The proof is completed. $\square$

For signs of τ_{12}, τ_{13} and τ_{23}, we now establish the following results.

Theorem 3.1. *Assume $m_l<m_r$ and $\sigma_{10}=\overline{\sigma_{20}}=iy$ with $y>0$. One has $\tau_{13}<0$ for any $(\alpha_1,\alpha_2)\in\Delta$. Furthermore,*

(i) if $V\geq V_{23}^*$, then $\tau_{23}<0$ for any $(\alpha_1,\alpha_2)\in\Delta$;

if $V<V_{23}^*$, then $\tau_{23}>0$ for $\alpha_1<\theta_{23}$ and $\alpha_2<P_{23}(\alpha_1)$; $\tau_{23}<0$ for $\alpha_1>\theta_{23}$ or $\alpha_2>P_{23}(\alpha_1)$;

(ii) if $y\kappa-z_3\zeta\geq0$, then $\tau_{12}<0$ for any $(\alpha_1,\alpha_2)\in\Delta$;

if $y\kappa-z_3\zeta<0$ and $M_{12}(V-V_{12}^*)<0$, then $\tau_{12}>0$ for any $(\alpha_1,\alpha_2)\in\Delta$;

if $y\kappa-z_3\zeta<0$ and $M_{12}(V-V_{12}^*)>0$, then $\tau_{12}<0$ for $\alpha_1<\theta_{12}$ and $\alpha_2<P_{12}(\alpha_1)$; $\tau_{12}>0$ for $\alpha_1>\theta_{12}$ or $\alpha_2>P_{12}(\alpha_1)$.

Proof. By (3.11) and Lemma 3.7, one has $V(y\kappa-z_2\zeta)>0$ and $\theta_{13}<0$. It follows from Theorem 3.2 that $\tau_{13}<0$ for any $(\alpha_1,\alpha_2)\in\Delta$.

Note that $V(y\kappa-z_2\zeta)>0$. If $V\geq V_{23}^*$, then one has from Lemma 3.6 that $\theta_{23}<0$. It then follows from (ii) in Theorem 3.2 that $\tau_{23}<0$. If $V<V_{23}^*$, then one has from Lemma 3.6 that $\theta_{23}>0$. It then follows from (ii) in Theorem 3.2 that $\tau_{23}>0$ for $\alpha_1<\theta_{23}$ and $\alpha_2<P_{23}(\alpha_1)$; $\tau_{23}<0$ for $\alpha_1>\theta_{23}$ or $\alpha_2>P_{23}(\alpha_1)$. The other cases can be obtained similarly. $\square$

It is obvious that τ_{12} (resp. τ_{23}) is continuous on Δ and the sign of τ_{12} (resp. τ_{23}) changes at $(\alpha_1,P_{12}(\alpha_1))$ (resp. $(\alpha_1,P_{23}(\alpha_1))$). Note that graphs of P_{ij}'s do not intersect (Proposition 3.10 in [57]).

Corollary 3.1. *Assume $m_l < m_r$ and $\sigma_{10} = \overline{\sigma_{20}} = iy$ with $y > 0$. If $V < V_{23}^*$, $y\kappa - z_3\zeta < 0$ and $M_{12}(V - V_{12}^*) > 0$, then*

(i) $\tau_{12} < \tau_{13} < 0 < \tau_{23}$ *for* $\alpha_1 < \theta_{23}$ *and* $\alpha_2 < P_{23}(\alpha_1)$;

(ii) $\tau_{13} < \tau_{12}(\tau_{23}) < 0$ *for* $P_{23}(\alpha_1) < \alpha_2 < P_{12}(\alpha_1)$ *or* $\theta_{23} < \alpha_1 < \alpha_2 < P_{12}(\alpha_1)$;

(iii) $\tau_{23} < \tau_{13} < 0 < \tau_{12}$ *for* $\alpha_1 > \theta_{12}$ *or* $\alpha_2 > P_{12}(\alpha_1)$.

Proof. For $V < V_{23}^*$, $y\kappa - z_3\zeta < 0$ and $M_{12}(V - V_{12}^*) > 0$, one has from Lemmas 3.6 and 3.7 that $\theta_{12} > \theta_{23} > 0$. Note that $\tau_{13} = \tau_{12} + \tau_{23} < 0$. The conclusion then follows from Theorem 3.1 directly. $\qquad\square$

4   Conclusion

In this work, for ionic flow involving three ion species (two cations with different valences and one anion), we continued the study in [57] on effects of permanent charges on ionic fluxes.

For the new case examined here, our results are consistent with some found in [57]. For the case of pure imaginary eigenvalues, one always has $\tau_{13} < 0$ though. Otherwise, the results in the new case study continue to support our conjectures raised in Section 5 of [57]; that is, we believe that the answers to the following questions are negative:

Question 1. Can $\tau_{13} > 0$ and $\tau_{23} > 0$ occur simultaneously?
Question 2. Can $\tau_{12} > 0$ and $\tau_{23} > 0$ occur simultaneously?

It is a common view that, if an ionic mixture consists of only one cation and one anion ion species, the ionic mixture behaves close to the salt in the sense that the concentrations of the cation and anion are tightly related due to electroneutrality nearly everywhere. On the other hand, with an additional ion species (another cation in this work), there is an extra freedom—the specifics (such as location characters α_1 and α_2) of permanent charges could coordinate two cation species using their boundary conditions to create behaviors far richer than what one may naively guessed (This was indeed happened to the authors several times when [57] and this paper were prepared). How much does this extra freedom allow one to do? The two case studies in [57] and this paper have shown a number of generally unexpected phenomena. The two questions raised in [57] and reiterated above concern limitations of this extra freedom, just like the universality for the case of two ion species in (1.9). We hope in the near future, answers to these questions could be available. We believe that our case studies, by no means trivial, could stimulate further investigation on these problems and other extensions.

We remark that, if the two cation species have the same valence, then their flux ratios are the same. This result, as a special case of a general result, will appear in a forthcoming paper.

Acknowledgements

References

 [1] Abaid N, Eisenberg R S, Liu W. Asymptotic expansions of I-V relations via a Poisson-Nernst-Planck system. SIAM J. Appl. Dyn. Syst., 2008, 7: 1507-1526.
 [2] Barcilon V. Ion flow through narrow membrane channels: Part I. SIAM J. Appl. Math., 1992, 52: 1391-1404.
 [3] Barcilon V, Chen D, Eisenberg R. Ion flow through narrow membrane channels: Part II. SIAM J. Appl. Math., 1992, 52: 1405-1425.
 [4] Barcilon V, Chen D, Eisenberg R, et al. Qualitative properties of steady-state Poisson-Nernst-Planck systems: Perturbation and simulation study. SIAM J. Appl. Math., 1997, 57: 631-648.
 [5] Bates P, Wen Z, Zhang M. Small permanent charge effects on individual fluxes via Poisson¨CNernst¨CPlanck models with multiple cations. J. Nonlinear Sci., https://doi.org/10.1007/s00332-021-09715-3.
 [6] Bazant M, Chu K, Bayly B. Current-Voltage relations for electrochemical thin films. SIAM J. Appl. Math., 2005, 65: 1463-1484.
 [7] Bezanilla F. The voltage sensor in voltage-dependent ion channels. Phys. Rev., 2000, 80: 555-592.
 [8] Bikerman J J. Structure and capacity of the electrical double layer. Philos. Mag., 1942, 33: 384-397.
 [9] Chen D P, Eisenberg R S. Charges, currents and potentials in ionic channels of one conformation. Biophys. J., 1993, 64: 1405-1421.
[10] Chen J, Wang Y, Zhang L, et al. Mathematical analysis of Poisson-Nernst-Planck models with permanent charges and boundary layers: studies on individual fluxes. Nonlinearity, 2021, 34(6): 3879-3906.
[11] Eisenberg R S. Channels as enzymes: oxymoron and taytology. J. Memb. Biol., 1990, 115: 1-12.
[12] Eisenberg B. Ion channels as devices. J. Comp. Electro., 2003, 2: 245-249.
[13] Eisenberg B. Proteins, channels, and crowded Ions. Biophys. Chem., 2003, 100: 507-517.
[14] Eisenberg B. Ions in fluctuating channels: transistors alive. Fluctuation and Noise Letters, 2012, 11: 1240001
[15] Eisenberg B, Hyon Y, Liu C. Energy variational analysis of ions in water and channels: Field theory for primitive models of complex ionic fluids. J. Chem. Phys., 2010, 133(1-23): 104104.
[16] Eisenberg B, Liu W. Poisson-Nernst-Planck systems for ion channels with permanent charges. SIAM J. Math. Anal., 2007, 38: 1932-1966.
[17] Eisenberg B, Liu W, Xu H. Reversal permanent charge and reversal potential: case studies via classical Poisson-Nernst-Planck models. Nonlinearity, 2015, 28: 103-128.

[18] Gillespie D, Nonner W, Eisenberg R S. Coupling Poisson-Nernst-Planck and density functional theory to calculate ion flux. J. Phys.: Condens. Matter, 2002, 14: 12129-12145.

[19] Gillespie D, Nonner W, Eisenberg R S. Density functional theory of charged, hard-sphere fluids. Phys. Rev. E, 2003, 68(1-10): 0313503.

[20] Gillespie D, Nonner W, Eisenberg R S. Crowded charge in biological ion channels. Nanotech., 2003, 3: 435-438.

[21] Hille B. Ion Channels of Excitable Membranes(3rd ed). Sinauer Associates Inc., 2001.

[22] Hodgkin A L. The ionic basis of electrical activity in nerve and muscle. Biol. Rev., 1951, 26: 339-409.

[23] Hodgkin A L, Huxley A F. Currents carried by sodium and potassium ions through the membrane of the giant axon of Loligo. J. Physol., 1952, 116: 449-472.

[24] Hodgkin A L, Huxley A F, Katz B. Ionic currents underlying activity in the giant axon of the squid. Arch. Sci. Physiol., 1949, 3: 129-150.

[25] Hodgkin A L, Katz B. The effect of sodium ions on the electrical activity of the giant axon of the squid. J. Physiol., 1949, 108: 37-77.

[26] Hodgkin A L, Keynes R. The potassium permeability of a giant nerve fibre. J. Physiol., 1955, 128: 61-88.

[27] Huang W, Liu W, Yu Y. Permanent charge effects on ionic flow: a numerical study of flux ratios and their bifurcation. Commun. Comput. Phys., 2021, 30: 486-514.

[28] Hyon Y, Eisenberg B, Liu C. A mathematical model for the hard sphere repulsion in ionic solutions. Commun. Math. Sci., 2010, 9: 459-475.

[29] Im W, Beglov D, Roux B. Continuum solvation model: Electrostatic forces from numerical solutions to the Poisson-Boltzmann equation. Comp. Phys. Comm., 1998, 111: 59-75.

[30] Im W, Roux B. Ion permeation and selectivity of OmpF porin: a theoretical study based on molecular dynamics, Brownian dynamics, and continuum electrodiffusion theory. J. Mol. Biol., 2002, 322: 851-869.

[31] Ji S, Eisenberg B, Liu W. Flux ratios and channel structures. J. Dynam. Differ. Eq., 2019, 31: 1141-1183.

[32] Ji S, Liu W. Poisson-Nernst-Planck systems for ion flow with density functional theory for hard-sphere potential: I-V relations and critical potentials. Part I: Analysis. J. Dynam. Differ. Eq., 2012, 24: 955-983.

[33] Ji S, Liu W, Zhang M. Effects of (small) permanent charge and channel geometry on ionic flows via classical Poisson-Nernst-Planck models. SIAM J. Appl. Math., 2015, 75: 114-135.

[34] Kilic M S, Bazant M Z, Ajdari A. Steric effects in the dynamics of electrolytes at large applied voltages. II. Modified Poisson-Nernst-Planck equations. Phys. Rev. E, 2007, 75(1-11): 021503.

[35] Li B. Continuum electrostatics for ionic solutions with non-uniform ionic sizes. Nonlinearity, 2009: 811-833.

[36] Lin G, Liu W, Yi Y, et al. Poisson-Nernst-Planck systems for ion flow with a local hard-sphere potential for ion size effects. SIAM J. Appl. Dyn. Syst., 2013, 12: 1613-1648.

[37] Liu J-L, Eisenberg B. Molecular mean-field theory of ionic solutions: a Poisson-Nernst-Planck-Bikerman model. Entropy, 2020, 22(5): 550.

[38] Liu J-L, Xie D, Eisenberg B. Poisson-Fermi formulation of nonlocal electrostatics in electrolyte solutions. Mol. Based Math. Biol., 2017, 5: 116-124.

[39] Liu W. Geometric singular perturbation approach to steady-state Poisson-Nernst-Planck systems. SIAM J. Appl. Math., 2005, 65: 754-766.

[40] Liu W. One-dimensional steady-state Poisson-Nernst-Planck systems for ion channels with multiple ion species. J. Differ. Eq., 2009, 246: 428-451.

[41] Liu W. A flux ratio and a universal property of permanent charges effects on fluxes. Comput. Math. Biophys., 2018, 6: 28-40.

[42] Liu W, Tu X, Zhang M. Poisson-Nernst-Planck systems for ion flow with density functional theory for hard-sphere potential: I-V relations and critical potentials. Part II: Numerics. J. Dynam. Differ. Eq., 2012, 24: 985-1004.

[43] Liu W, Wang B. Poisson-Nernst-Planck systems for narrow tubular-like membrane channels. J. Dynam. Differ. Eq., 2010, 22: 413-437.

[44] Liu W, Xu H. A complete analysis of a classical Poisson-Nernst-Planck model for ionic flow. J. Differ. Eq., 2015, 258: 1192-1228.

[45] Mofidi H, Eisenberg B, Liu W. Effects of diffusion coefficients and permanent charge on reversal potentials in ionic channels. Entropy, 2020, 22(1-23): 325.

[46] Mofidi H, Liu W. Reversal potential and reversal permanent charge with unequal diffusion coefficients via classical Poisson-Nernst-Planck models. SIAM J. Appl. Math., 2020, 80: 1908-1935.

[47] Nonner W, Eisenberg R S. Ion permeation and glutamate residues linked by Poisson-Nernst-Planck theory in L-type calcium channels. Biophys J, 1998, 75: 1287-1305.

[48] Park J-K, Jerome J W. Qualitative properties of steady-state Poisson-Nernst-Planck systems: Mathematical study. SIAM J. Appl. Math., 1997, 57: 609-630.

[49] Rosenfeld Y. Free-energy model for the inhomogeneous hard-sphere fluid mixture and Density-Functional theory of freezing. Phys. Rev. Lett., 1989, 63: 980-983.

[50] Rosenfeld Y. Free energy model for the inhomogeneous fluid mixtures: Yukawa-charged hard spheres, general interactions, and plasmas. J. Chem. Phys., 1993, 98: 8126-8148.

[51] Rubinstein I. Electro-Diffusion of Ions. SIAM Studies Appl. Math., 1990, 11: 203-249.

[52] Sakmann B, Neher E. Single Channel Recording (2nd Ed.). Plenum, 1995.

[53] Schmidt M, Löwen H, Brader J M, et al. Density functional theory for a model colloid-polymer mixture: Bulk fluid phases. J. Phys.: Condens. Matter, 2002, 14: 9353-9382.

[54] Singer A, Norbury J. A Poisson-Nernst-Planck model for biological ion channels–an asymptotic analysis in a three-dimensional narrow funnel. SIAM J. Appl. Math., 2009, 70: 949-968.

[55] Singer A, Gillespie D, Norbury J, et al. Singular perturbation analysis of the steady-state Poisson-Nernst-Planck system: applications to ion channels. European J. Appl. Math., 2008, 19: 541-560.

[56] Sun L, Liu W. Non-localness of excess potentials and boundary value problems of Poisson-Nernst-Planck systems for ionic flow: a case study. J. Dynam. Differ. Eq., 2018, 30: 779-797.

[57] Sun N, Liu W. Flux ratios for effects of permanent charges on ionic flows with three ion species: New phenomena from a case study. J. Dynam. Differ. Eq., 2024, 36: 27-62.

[58] Tarazona P, Rosenfeld Y. From zero-dimension cavities to free-energy functionals for hard disks and hard spheres. Phys. Rev. E, 1997, 55: R4873-R4876.

[59] Ussing H H. The distinction by means of tracers between active transport and diffusion. Acta Physiol. Scand., 1949, 19: 43-56.

[60] Ussing H H. Interpretation of the exchange of radio-sodium in isolated muscle. Nature, 1947, 160: 262-263.

[61] Wang X-S, He D, Wylie J, et al. Singular perturbation solutions of steady-state Poisson¨CNernst¨CPlanck systems. Phys. Rev. E, 2014, 89: 022722.

[62] Wei G-W, Zheng Q, Chen Z, et al. Variational multiscale models for charge transport. SIAM Rev., 2012, 54: 699-754.

[63] Wen Z, Zhang L, Zhang M. Dynamics of classical Poisson-Nernst-Planck systems with multiple cations and boundary layers. J. Dynam. Differ. Eq., 2021, 33: 211-234.

[64] Yan L, Xu H, Liu W. Poisson-Nernst-Planck models for three ion species: Monotonic profiles vs. oscillatory profiles. J. Appl. Anal. Comput., 2022, 12: 1211-1233.

[65] Zhang L, Eisenberg B, Liu W. An effect of large permanent charge: decreasing flux with increasing transmembrane potential. Eur. Phys. J. Special Topics, 2019, 227: 2575-2601.

[66] Zhang L, Liu W. Effects of large permanent charges on ionic flows via Poisson-Nernst-Planck models. SIAM J. Appl. Dyn. Syst., 2020, 19: 1993-2029.

[67] Zhang M. Competition between cations via classical Poisson-Nernst-Planck models with nonzero but small permanent charges. Membranes, 2021, 11(4): 236.